

Supplemental Information

A Critical Role for Notch Signaling

in the Formation of Cholangiocellular Carcinomas

Steffen Zender, Irina Nickeleit, Torsten Wuestefeld, Inga Sörensen, Daniel

Dauch, Przemyslaw Bozko, Mona El-Khatib, Robert Geffers, Hueseyin Bektas,

Michael P. Manns, Achim Gossler, Ludwig Wilkens, Ruben Plentz, Lars Zender,

and Nisar P. Malek

Inventory of Supplemental Information

Supplemental Data

Figure S1 related to Figure 1

Figure S2 related to Figure 3

Figure S3 related to Figure 5

Table S1 related to Figure 5

Figure S4 related to Figure 6

Supplemental Experimental Procedures

Supplemental References

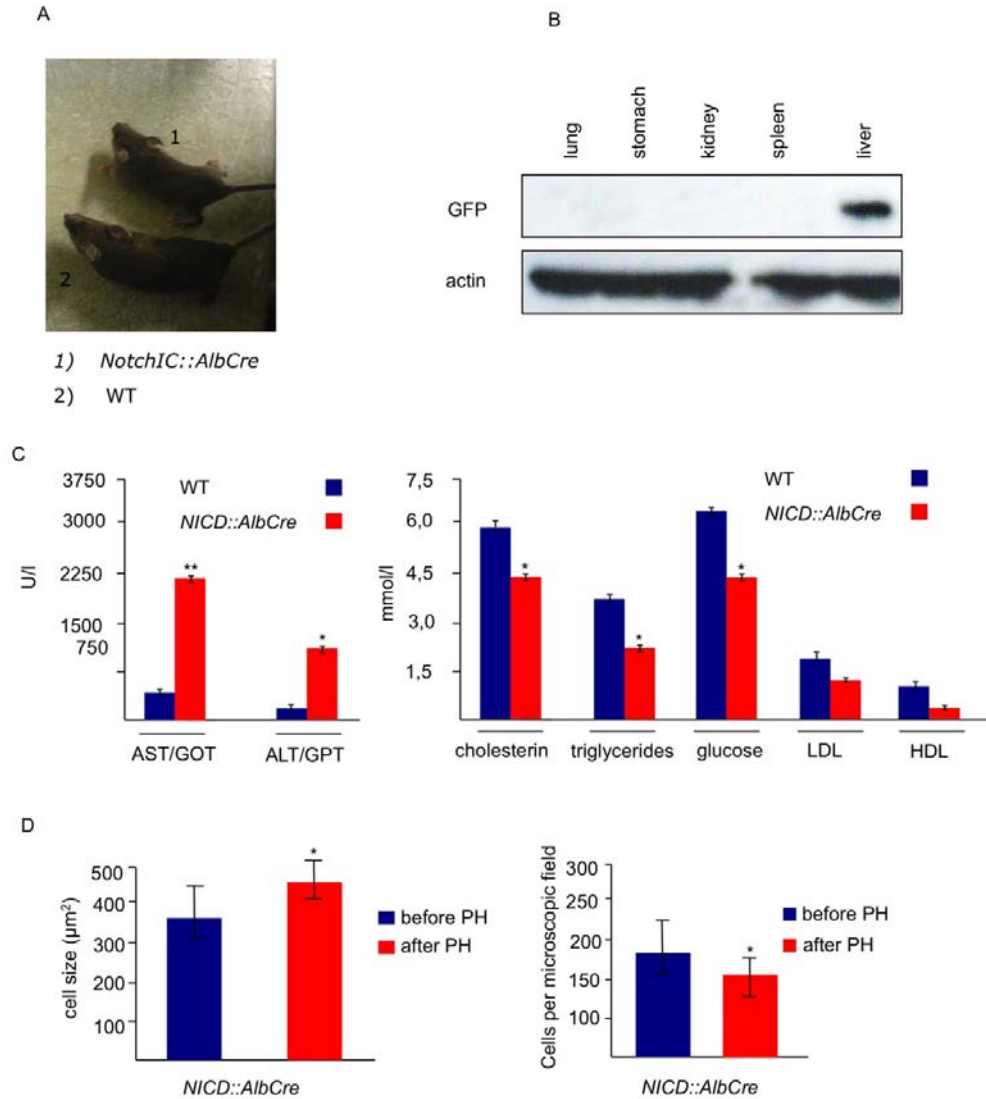


Figure S1 related to Figure 1 A. Growth differences of *NotchIC::AlbCre* mice and WT littermates at seven months of age. B. Western blot analysis of various organs to measure GFP expression (10 week old mice). C. Quantification of serum transaminases and different liver metabolites in *NICD::AlbCre* and WT littermates (age of 12 weeks). D. Quantification of cell size and the number of cells per microscopic field before and after performing partial hepatectomies (4 days post ph)

in *NICD::AlbCre* and WT littermates. Scale bars represent mean values \pm SEM.

Asterisk denotes significance levels * $p < 0.05$; ** $p < 0.001$.

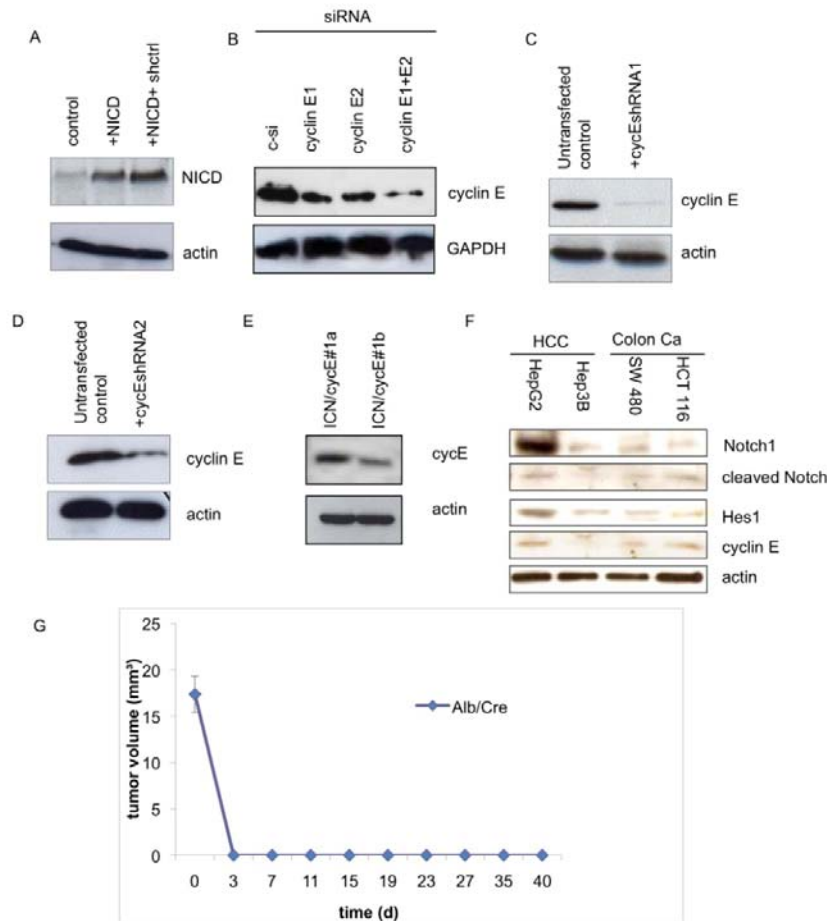


Figure S2 related to Figure 3

A. Mouse bipotential liver progenitor cells were infected with retroviral vectors to stably overexpress NICD. Vector infected cells served as controls. Shown are the expression levels of NICD in such cells compared to empty vector infected cells. B. Transfection of MzChA1 cholangiocarcinoma cells with a siRNA against Cyclin E1, E2 or both and determination of cyclin E knockdown by western blotting. C, D. We transduced NICD expressing liver progenitor cells with retroviruses for stable expression of two different shRNAs against Cyclin E. After selection, we

measured the knockdown level of cyclin E in these cell populations. E. Western blot analysis of tumor tissue derived from mouse 1a and 1b showed persistent cyclin E protein expression indicating that the tumors developed from cells without shRNA-cyclin E expression or from cells that may have silenced shRNA cyclin E expression. F. Western blot analysis of Notch1, cleaved Notch, Hes 1 and cyclin E in different hepatocellular and colon carcinoma cell lines. G. Liver tissue from *Alb-Cre* transgenic mice was minced and injected s.c. into immunodeficient mice.

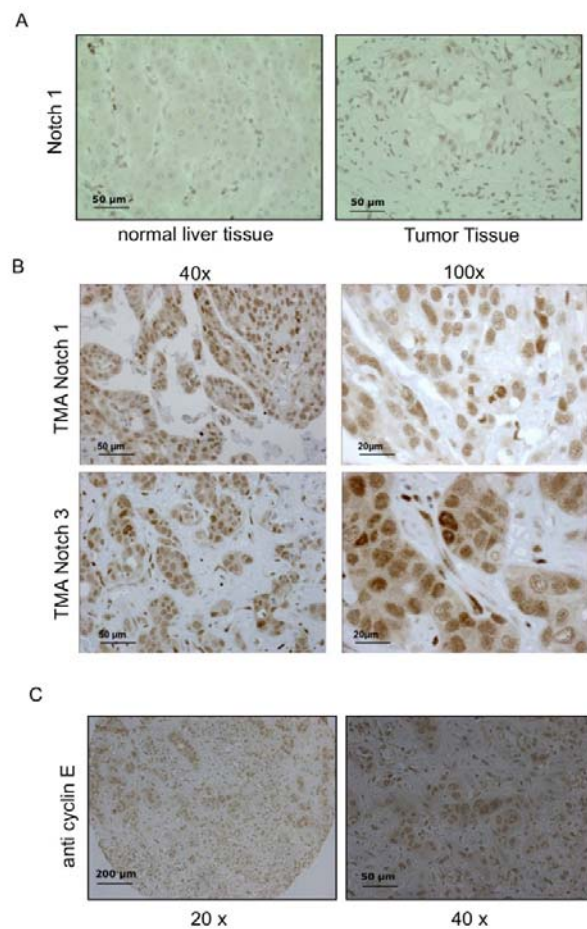


Figure S3 related to Figure 5

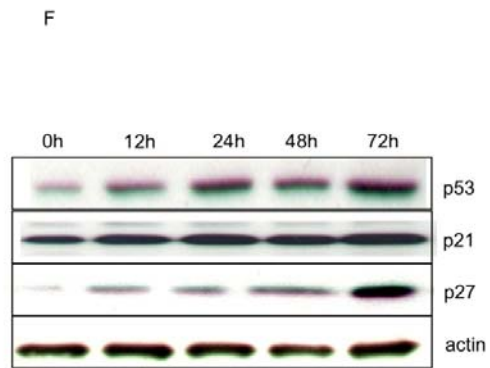
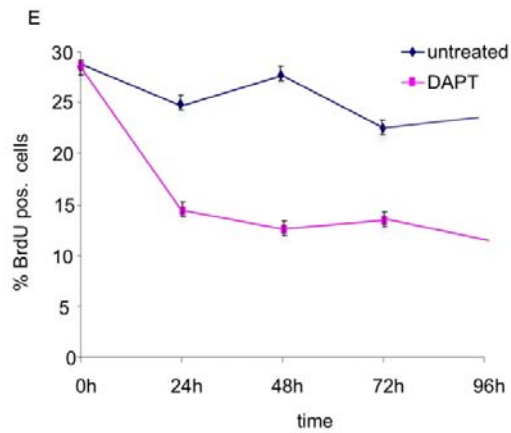
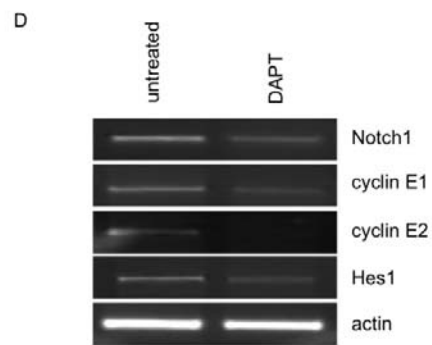
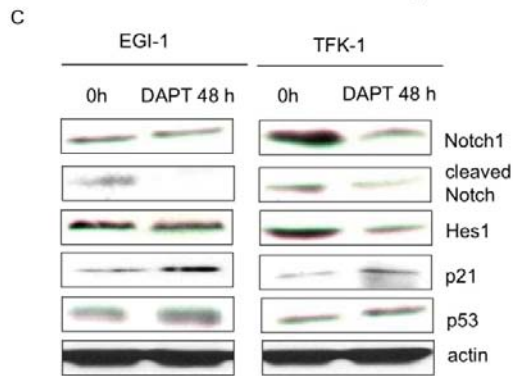
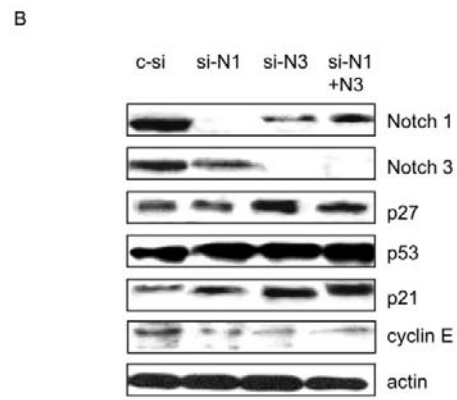
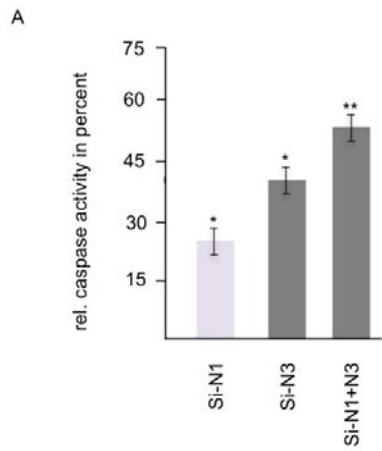
A. Wildtype liver tissue and tumor tissue from the same patient stained with Notch 1 antibody. The Notch 1 antibody stains intrahepatic lymphocytes. B. Higher

magnification of Notch 1 and Notch 3 expression in human cholangiocellular carcinoma. C. Representative anti-cyclin E staining in human CCC tissues using different magnifications.

Table S1 related to Figure 5 Characteristics of patients and tumors analyzed as part of the CCC tissue micro array.

nr.	gender	age	liver disease	tumor type	TNM	Grade	histology of surrounding liver tissue
1	male	71	-	Klatskin	T4 M1	G2-3	chronic cholangitis
2	fem.	60	-	distal DHC	T3 N1 Mx	G2	normal
3	male	62	-	intrahepatic	T3 N1 M1	G2-G3	normal
4	male	63	-	distal DHC	T1 N1 Mx	G1	normal
5	male	68	-	distal DHC	T4 M1	G2-G3	normal
6	male	67	-	Klatskin	T1 N1	G2	normal
7	fem.	44		Klatskin	T3 N1 Mx	G1	chronic cholangitis
8	fem.	74	-	intrahepatic	T3 N1 Mx	G1	cholestasis
9	fem.	79	-	intrahepatic	T3 N1 Mx	G2	normal
10	fem.	77	-	intrahepatic	T3 N1 M1	G2	biliary hamartoma, chronic hepatitis
11	fem.	62	NASH	intrahepatic	T3 N1 Mx	G2-G3	normal
12	male	69	-	intrahepatic	T3 N1 Mx	G2	bile duct papillomatosis
13	male	70	-	distal DHC	T3 N1 Mx	G2-G3	normal
14	male	62	-	intrahepatic	T3 N1 M1	G3	chronic cholestasis
15	male	49	-	intrahepatic	T3 N1 M!	G3	hemosiderosis
16	male	56	NASH	intrahepatic	T3 N1 Mx	G2	steatosis
17	fem.	56	-	intrahepatic	T3 N1 Mx	-	hemosiderosis, steatosis
18	fem.	81	-	intrahepatic	T3 N1 Mx	G3	hemosiderosis
19	fem.	30	PSC	intrahepatic	T3 N1 M1	G2	normal
20	male	58	-	distal DHC	T3 N1 Mx	-	chronic cholangitis
21	fem.	75	Mirizzi syndrome	gall bladder	T3 N1	G3	normal
22	fem.	53	-	intrahepatic	T3 N1 Mx	G3	normal
23	fem.	33	-	intrahepatic	T3 N1 M1	G2-G3	fibrosis
24	fem.	59	-	gall bladder	T2 N1	-	normal
25	male	76	-	intrahepatic	T3 N1 Mx	G2-G3	chronic

							cholestasis
26	fem.	70	-	distal DHC	T3 N1 Mx	G2	chronic cholestasis, fibrosis
27	male	49	-	intrahepatic	T3 N1 M1	-	NASH
28	fem.	49	-	intrahepatic	T2 N1 Mx	G2 -G3	NASH
29	male	65	-	intrahepatic	T2 N1 Mx	G3	ASH
30	male	31	PSC	Klatskin	T1 N1 Mx	G1	fibrosis
31	male	70	-	Klatskin	T2 N1 Mx	G2	normal
32	male	67		Klatskin	T1 N1 Mx	G1	cholestasis
33	male	59	-	Klatskin	T2 N1 Mx	G3	cholestasis
34	male	65	-	intrahepatic	T4 N1	-	
35	fem.	64	-	intrahepatic	T2 N1 Mx	G2	NASH
36	fem.	79	-	intrahepatic	T3 N1 M1	G3	steatosis
37	fem.	56	-	intrahepatic	T2 N1	-	steatosis
38	fem.	68	-	Klatskin	T3 N1 Mx	G3	fibrosis
39	fem.	66	-	intrahepatic	T3 N1 M1	-	steatosis
40	male	80	Hepatitis C	intrahepatic	T4 M1	G3	biliary fibrosis
41	male	77	-	intrahepatic	T3 N1 Mx	G2-G3	normal
42	fem.	59	-	Klatskin	T3 N1	G2-G3	normal
43	male	63	-	intrahepatic	T3 N1	-	steatosis
44	fem.	65	-	intrahepatic	T3 N1 Mx	G2-G3	steatosis
45	male	61	-	intrahepatic	T2 N1	G2	NASH
46	fem.	62	-	intrahepatic	T2 N1	G3	NASH
47	male	76	-	distal DHC	T2 N1	G3	hemosiderosis
48	male	60	-	intrahepatic	T3 N1 Mx	G2-G3	steatosis
49	male	21	PSC	Klatskin	T1 N0	-	normal
50	male	59	-	Klatskin	T1 N0	G2	fibrosis
51	male	64	alpha 1 antitrypsin deficiency	intrahepatic	T3 N1 Mx	-	zirrrosis
52	male	71	-	intrahepatic	T2 N1	G2	normal
53	fem.	56	-	intrahepatic	T2 N1	G2	steatosis
54	fem.	81	-	intrahepatic	T2 N1	G2	normal
55	male	86	-	intrahepatic	T3 N1 Mx	G2-G3	steatosis
56	fem.	73	Hepatitis C	distal DHC	T2 N1	G2-G3	cirrhosis



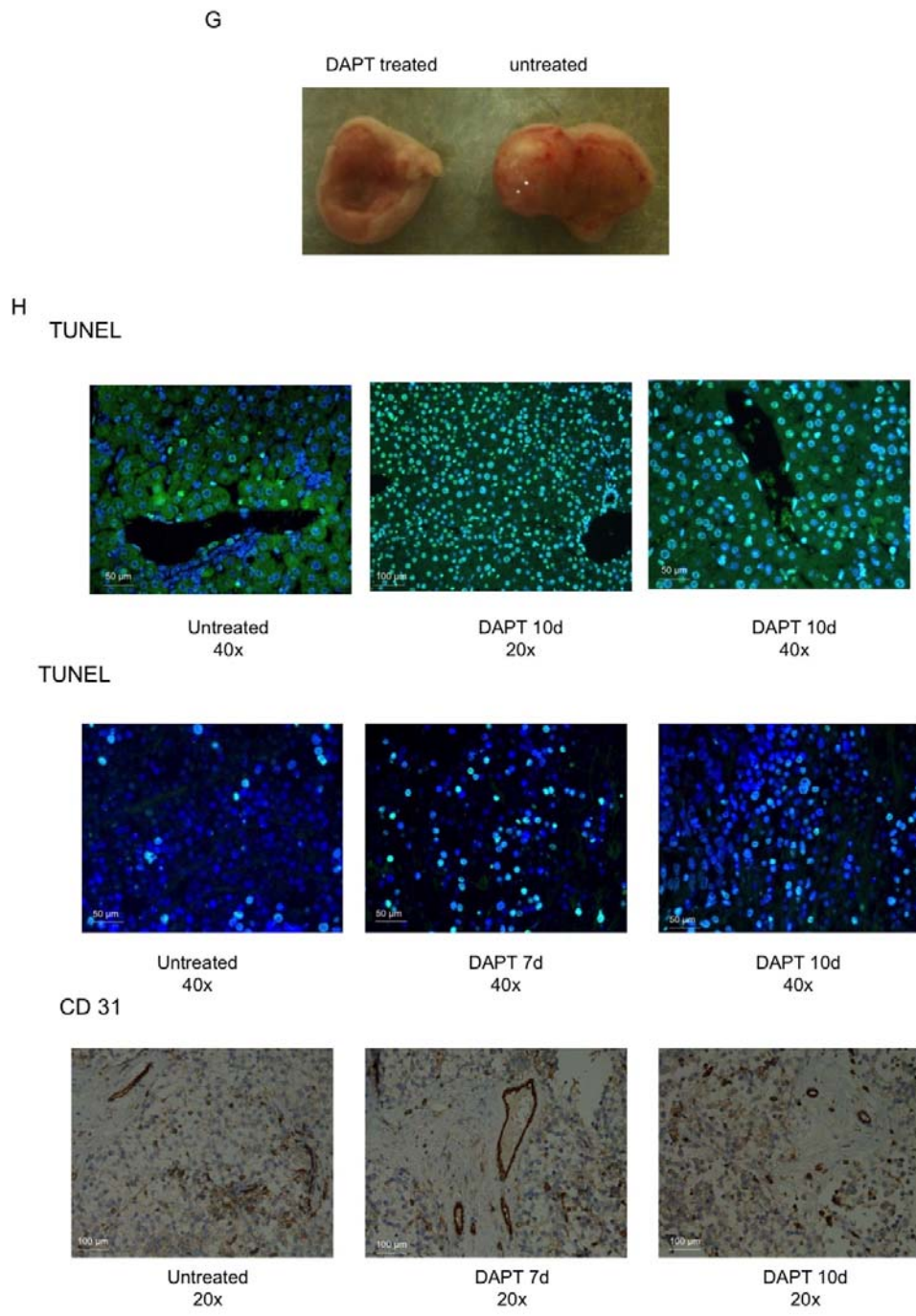


Figure S4 related to Figure 6

A. Relative caspase activity of MzChA1 cells after siRNA mediated knockdown of Notch1, Notch3 or both. B. Western blot expression analysis of p53, p27, p21 and

cyclin E after after siRNA mediated knockdown (after 48h) of Notch1, Notch3 or both. C. Western Blot analysis of Notch1, cleaved Notch, Hes 1, p21, p27 and p53 before and after DAPT (10 μ M) treatment in two other cholangiocellular carcinoma cell lines (EGI1, TFK1). D. Comparison of the expression levels of activated Notch1, cyclin E1, cyclin E2 and HES 1 mRNA with and without DAPT treatment (38,7 μ M) for 48 h. E. Graphical display of BrdU positive CCC cells with and without DAPT treatment (10 μ M). F. MzChA1 cells were treated with DAPT (10 μ M) for the indicated times. Expression of p53, p27 and p21 was determined by western blot analysis. Scale bars represent mean values \pm SEM. G. Liver tissue from Albumin Cre transgenic mice was injected s.c. into immunodeficient mice. The graph shows that this tissue is not able to form tumors. G. Representative pictures of treated and untreated xenotransplanted human CCC tumors. H. Xenotransplanted tumors were stained with the help of the InSituCellDeath Detection Kit. Shown are different timepoints after null, seven and ten days of DAPT treatment. Mouse tumor tissues were stained with anti CD31 antibodies to visualize endothelial cells.

Supplemental Experimental Procedures

Generation of immortalized bipotential liver progenitor cells, retroviral transduction and subcutaneous injection of cells

Cells were subjected to controlled immortalization by retroviral transduction with a microRNA based shRNA targeting p16INK4/p19Arf (CCGCTGGGTGCTCTTTGTGTT, targeted mRNA sequence).

Full length ICN cDNA was amplified from pCS2+ (Mumm et al., 2000) using PCR primers with EcoRI overhangs and subsequently cloned into an EcoRI digested MSCV-Puro (Clontech) vector. MicroRNA based shRNAs targeting murine cyclin E (1043, 981, numbers indicate starting point of the 21bp mRNA targeting positions) were obtained from Open Biosystems and subcloned into a modified MSCV-Hygromycin vector (Clontech). Production of retroviral particles and target cell transduction was performed as described recently (Zender et al., 2008) Cells were selected with puromycin or hygromycin and 6×10^6 cells were injected subcutaneously in the rear flanks of NMRI nu/nu mice. Tumor growth was quantified using standard caliper measurement and tumor volume was calculated by the following formula: $(\text{length} \times [\text{width}^2]) \times \pi/6$.

Generation of cell lines and xenotransplant studies

Human tumor tissue obtained after resection of a primary intrahepatic cholangiocellular carcinoma was dissected and minced carefully with sterile instruments. Afterwards the tissue was digested for 45 minutes in 0.125% collagenase type 1 dissolved in M199 Hanks salt buffered and sterile filtered with aerating/bubbling at 37°C. A vial was placed on ice to precipitate tissue for

minutes. The supernatant was discarded, 4 ml of medium was added and filtered through 40µm mesh before plating of cells into tissue culture plates.

Generally 1×10^7 cells mixed with 100 µl DMEM and 100 µl Matrigel were injected subcutaneously into the flanks of NMRI nu/nu mice. Tumors grew for approximately 21 days until they reached an appropriate size (150-200 mm³). Tumor size was measured with a digital caliper and calculated with the help of the following formula: $(\text{length} \times [\text{width}^2]) \times \pi/6$. When xenotransplanted tumors reached a size of approximately 150-200 mm³ mice were treated with DAPT at a concentration of 50 mg/kg i.p. every 72 hours.

siRNA

cyclin E1; Hs -CCNE 1-5; NM 001238:

sense: 5'-GAAGAGUAUUAAAUAUAUATT-3';

antisense: 5'-UAUAUAUUUAAUACUCUUCTT-3';

cyclin E 2: Hs-ccNE2-7:

sense: 5'-GAAGAGUAUUAAAUAUAUATT-3';

antisense: 5'-UAUAUAUUUAAUACUCUUCTT-3 from Qiagen.

Immunohistochemistry

BrdU labeling in mice was done by injecting 10 µl/g BrdU solution i.p. two hours before sacrificing the mice, BrdU staining of 6 µm cryostat sections was done as described (Satyanarayana et al., 2003). The BrdU labeling index was determined by counting the number of BrdU-positive cells in 25 low-power (10x) magnification fields chosen at random and expressing the number of BrdU-labeled nuclei as percentage of all nuclei counted. At least 4 sections and 4 visual fields of each collected sample were quantified. Antibodies used in

immunohistochemistry were: Cleaved Notch 1 (ab 8925), Hes 1 (ab 49170), cyclin E [12A3] (ab 9517) (all Abcam), β -catenin (BD Transduction Laboratories), CD 34 (8158) Abcam. Immunohistochemical stainings of tissue sections were done using the following antibodies against Notch receptors: Notch1 (H131), SC 9170 □ Notch 2 (25-255), SC-5545 □ Notch 3 (M134), SC-5593 □ Notch 4 (H225), SC-5594 (all Santa Cruz)

Staining was performed on paraffin sections after boiling the sections in Tris-EDTA (pH 9.0) for 20 minutes. After blocking the slides with 1% BSA/PBS for 1 h, the antibody was incubated for 2 h in PBS/0.05 % BSA.

Morphological analysis of immunohistochemical stainings for the antibodies mentioned above in tissue sections of paraffin embedded tumour specimens including the tissue microarrays was done semiquantitatively. For this purpose nuclear and/or cytoplasmatic stainings were classified as weak (score 1) when faint staining was detectable in a magnification of at least 10x10. Moderate staining (score 2) was assumed when a clearly detectable staining was occurring. A strong staining (score 3) was defined as a dense staining already detectable in scanning magnification (2.5x10).

Nuclei positive for HH3 phosphorylation were detected using an anti-HH3 antibody (Cell signalling), and analysis was performed as described (Brenner et al. 2003).

For γ H2AX staining (γ H2AX antibody, Upstate Biotechnology) sections were deparaffinized and antigen retrieval was performed in 10mM citrate buffer pH 6.0. For detection of apoptosis we used the Caspase-Glo ® 3/7 Assay from Promega according to the manufacturer's instructions.

Supplemental References

Mumm, J. S., Schroeter, E. H., Saxena, M. T., Griesemer, A., Tian, X., Pan, D. J., Ray, W. J., and Kopan, R. (2000). A ligand-induced extracellular cleavage regulates gamma-secretase-like proteolytic activation of Notch1. *Mol Cell* 5, 197-206.

Satyanarayana, A., Wiemann, S. U., Buer, J., Lauber, J., Dittmar, K. E., Wustefeld, T., Blasco, M. A., Manns, M. P., and Rudolph, K. L. (2003). Telomere shortening impairs organ regeneration by inhibiting cell cycle re-entry of a subpopulation of cells. *Embo J* 22, 4003-4013.

Zender, L., Xue, W., Zuber, J., Semighini, C. P., Krasnitz, A., Ma, B., Zender, P., Kubicka, S., Luk, J. M., Schirmacher, P., *et al.* (2008). An oncogenomics-based in vivo RNAi screen identifies tumor suppressors in liver cancer. *Cell* 135, 852-864.